RSC Advances

COMMUNICATION

View Article Online
View Journal | View Issue

Inertial rise in short capillary tubes

Cite this: *RSC Adv.*, 2014, **4**, 14781

Orest Shardt,*[a] Prashant R. Waghmare,[b] J. J. Derksen[a] and Sushanta K. Mitra[b]

Received 20th January 2014
Accepted 10th March 2014

DOI: 10.1039/c4ra00580e

www.rsc.org/advances

Published on 13 March 2014. Downloaded by University of Alberta on 11/05/2014 20:25:04.

The behavior of liquid that rises to the top of a short tube depends on the Weber number We defined as the ratio of the kinetic energy of the liquid and a reference surface energy. In optimal experiments with diethyl ether, the meniscus of the rising liquid inverts and spreads onto the external surface of the tube when $We \gtrsim 1$. If $We \lesssim 1$, the meniscus remains pinned at the top of the tube. For inertial capillary rise dynamics the maximum kinetic energy is achieved when the height of the liquid column is 3/4 of the equilibrium rise height and diverges with decreasing gravitational acceleration.

Though the phenomenon of capillary rise is generally well-understood, one aspect has received minimal attention: the behavior of the rising liquid when it reaches the top of a tube. First studied by Leonardo da Vinci in the fifteenth century,[1] capillary phenomena have since been investigated under a wide variety of conditions, including microgravity.[2–4] Drop towers provide brief periods of microgravity that are used, for example, to study capillary phenomena under conditions that are relevant to fluid systems in spacecraft. In their drop tower experiments, Siegel[2] and Wollman and Weislogel[4] found that the liquid briefly bulged out upon reaching the top of the tube, the edge of the bulge remained pinned, and the liquid then descended. Here we show in experiments under normal gravity that the previously-observed outcome in microgravity is not the only possible outcome: the liquid can also spread onto the external walls rather than remaining pinned at the top. This outcome seems unexpected because the higher gravitational acceleration in our experiments should presumably oppose the rise of the liquid and therefore prevent a large bulge from forming. In this communication, we present our experiments, explain the occurrence of the external wetting phenomenon, and answer several outstanding questions about the dynamics of capillary rise: What is the maximum kinetic energy of the liquid during its rise towards an equilibrium height? How does the maximum kinetic energy depend on the physical properties of the system (the viscosity, density, and surface tension of the liquid) and the experimental conditions? The answers to these questions reveal the limitations of Earth-bound experiments and suggest new possibilities for capillary phenomena in microgravity.

The dynamics of capillary rise are determined primarily by the balance between the inertia of the fluid, the capillary driving force, the weight of the liquid, and resisting viscous forces. Depending on the relative magnitudes of these forces, the height of the liquid column scales differently with time,[3,5,6] and the path of the meniscus towards its equilibrium position (the Jurin[7] height) may be monotonic[5,8,9] or oscillatory.[10,11] Oscillations occur when the viscous boundary layer develops relatively slowly, keeping viscous forces low during the rise, and leaving only gravity and liquid inertia to balance the capillary force. For diethyl ether (surface tension $\sigma = 16.6$ mN m^{-1}, density $\rho = 710$ kg m^{-3}, dynamic viscosity $\mu = 0.22$ mPa s, and kinematic viscosity $\nu = 3.1 \times 10^{-7}$ m^2 s^{-1} at 25 °C) in a 1 mm diameter capillary, the viscous boundary layer grows with a ~200 ms characteristic time scale.[10] This time scale is similar to the time needed to reach the equilibrium height, at which the difference in hydrostatic pressure between the top and bottom of the liquid column matches the Laplace pressure difference across the meniscus. As a result, the liquid initially exceeds the equilibrium height and oscillates until viscous forces stop the motion.[10] When viscous forces develop much faster than the time needed to reach the equilibrium height, they also contribute to the rise dynamics. The dynamics of capillary rise during its different regimes have been studied thoroughly by many authors,[5,6,8,9,12] among others.

For inertial filling dynamics, it is straightforward to determine the maximum kinetic energy of the rising liquid. Assuming a flat flow profile, a reasonable assumption for inertial flow, the instantaneous kinetic energy E_k of the rising liquid is

$$E_k = \frac{1}{2}\rho\pi R^2 h\left(\frac{dh}{dt}\right)^2, \quad (1)$$

[a]*Department of Chemical and Materials Engineering, University of Alberta, Edmonton, Alberta, T6G 2V4, Canada. E-mail: shardt@ualberta.ca*

[b]*Department of Mechanical Engineering, University of Alberta, Edmonton, Alberta, T6G 2G8, Canada*

Published on 13 March 2014. Downloaded by University of Alberta on 11/05/2014 20:25:04.

where R is the inner radius of the capillary tube, t is time, and h is the height of the liquid column from the base of the tube (the tubes do not penetrate into the liquid reservoir) to the bottom of the meniscus. Here and in later derivations we neglect the mass of the liquid in the meniscus ($\frac{1}{3}\rho\pi R^3$ for perfect wetting), a valid assumption in the limit of $h \gg R$ or a large contact angle. We note also that the average speed of the liquid is $\frac{dh}{dt}$ provided that the meniscus is not deforming, which is a reasonable assumption until the top of the meniscus reaches the top of the tube and the interface begins to invert. We compare the kinetic energy E_k with the reference surface energy $4\pi R^2\sigma$ to define a Weber number. This surface energy may be interpreted in two ways. It is the surface energy of a spherical drop with the same radius as the tube. It is also the work done on a column of liquid (of constant mass) by the Laplace force $(\pi R^2)(2\sigma/R)$ over the distance $2R$. Once the meniscus inverts at the top of the tube, this Laplace force pushes the liquid back into the tube while it continues to rise. The resulting Weber number is

$$\mathrm{We} = \frac{\rho}{8\sigma} h \left(\frac{dh}{dt}\right)^2. \quad (2)$$

Due to the use of $\frac{dh}{dt}$ as the average speed of the liquid in eqn (1), this Weber number only expresses the desired energy ratio until the top of the meniscus reaches the top of the capillary tube.

A simple governing equation for inertial rise dynamics in non-dimensional form is[10]

$$\frac{d}{d\tilde{t}}\left(\tilde{h}\frac{d\tilde{h}}{d\tilde{t}}\right) = 1 - \tilde{h}, \quad (3)$$

where the tildes indicate non-dimensional values, $\tilde{t} = t\sqrt{g/h_{eq}}$, $\tilde{h} = h/h_{eq}$, and $h_{eq} = 2\sigma/\rho g R$, where g is the gravitational acceleration. The solution for the height is

$$\tilde{h}(\tilde{t}) = \tilde{t}\left(1 - \frac{1}{6}\tilde{t}\right). \quad (4)$$

Consequently, the rise speed is

$$\frac{d\tilde{h}}{d\tilde{t}} = 1 - \frac{1}{3}\tilde{t}, \quad (5)$$

and the Weber number is

$$\mathrm{We} = \frac{1}{2\mathrm{Bo}}\tilde{t}\left(1 - \frac{1}{6}\tilde{t}\right)\left(1 - \frac{1}{3}\tilde{t}\right)^2, \quad (6)$$

where $\mathrm{Bo} = \rho g R^2/\sigma$ is the Bond number. It follows that the maximum We, denoted by We*, is $\frac{3}{16}\mathrm{Bo}^{-1}$. During the upward half of the parabolic trajectory (eqn (4)), the maximum is achieved when $\tilde{t}^* = 3(1 - 1/\sqrt{2})$, $\tilde{h}^* = 3/4$, and $\left(\frac{d\tilde{h}}{d\tilde{t}}\right)^* = \frac{1}{\sqrt{2}}$. For fixed fluid properties, We* diverges as $g \to 0$ or $R \to 0$.

For experiments on Earth (or any specific g), it would seem reasonable to pick successively smaller radii to investigate how the liquid that reaches the top of a tube behaves with increasing We*. However, decreasing the radius of the tube reduces the time required for a viscous boundary layer to develop, causing a transition to viscous filling dynamics. Adding the viscous force $8\pi\mu h\frac{dh}{dt}$, which assumes a fully-developed parabolic flow profile,[5,8,9,13] to eqn (3), we obtain

$$\frac{d}{d\tilde{t}}\left(\tilde{h}\frac{d\tilde{h}}{d\tilde{t}}\right) = 1 - \tilde{h} + 8\sqrt{2}\left(\frac{\mathrm{Oh}}{\mathrm{Bo}}\right)\tilde{h}\frac{d\tilde{h}}{d\tilde{t}}. \quad (7)$$

This equation has one non-dimensional parameter, the ratio of the Ohnesorge number ($\mathrm{Oh} = \nu\sqrt{\rho/(\sigma R)}$) and the previously-defined Bond number. The inertial model is obtained in the limit $\frac{\mathrm{Oh}}{\mathrm{Bo}} \to 0$. For room temperature diethyl ether in a 1.0 mm diameter capillary tube under terrestrial gravity, Bo ≈ 0.1, Oh ≈ 0.003, and $\frac{\mathrm{Oh}}{\mathrm{Bo}} \approx 0.03$. In contrast, for water, Bo ≈ 0.03, Oh ≈ 0.005, and $\frac{\mathrm{Oh}}{\mathrm{Bo}} \approx 0.15$. Among common liquids, diethyl ether is optimal (lowest Oh and therefore lowest Bo and highest We* for any $\frac{\mathrm{Oh}}{\mathrm{Bo}} \ll 1$), and we therefore used ether to achieve a high We* and ensure that the filling dynamics are inertial.

Since the capillary rise of diethyl ether under terrestrial conditions is not purely inertial (the oscillation dampens before a complete cycle[10,11]), the maximum Weber number occurs at a height less than $\tilde{h}^* = 3/4$. Experiments with 16 mm high borosilicate tubes with three different inner diameters (0.8, 0.9 and 1.0 mm) were therefore performed to determine the maximum Weber number and the height at which it is achieved. In these experiments, the bases of the capillary tubes contact a reservoir filled above its rim (as in ref. 5). To make contact, we raise the liquid level by inserting a pipette into the fluid instead of lowering the tube. In this arrangement, the meniscus inside the reservoir does not obstruct the view of the base of the tube, allowing us to observe the early stages of the rise. The experiments were backlit through a diffuser and recorded with a high-speed camera (Phantom v210, Vision Research, USA), capturing at 20 000 frames per second, with 30 μs exposure, and 29.3 μm per pixel (34.1 pixels per mm). The chosen magnification and frame rate allow good resolution of the interface motion: movement at the capillary speed $c = \sqrt{2\sigma/(\rho R)}$ corresponds to ≈0.3 pixels during the exposure time and ≈0.5 pixels during the time between the start of each exposure (inverse of the frame rate).

The experimental heights of the liquid column are compared with numerical solutions of eqn (7) in Fig. 1. Two experiments were performed with 0.8 mm diameter capillary tubes, and nearly indistinguishable results were obtained (Fig. 1a). The numerical results qualitatively capture the features of the oscillation despite the simplifying assumptions of the theoretical model. The most important assumption is that the liquid wets the glass tube perfectly (*i.e.* with zero contact angle). In the experiments, contact angles from ~40° at the start to ~10° at equilibrium were estimated from images of

 This journal is © The Royal Society of Chemistry 2014

Published on 13 March 2014. Downloaded by University of Alberta on 11/05/2014 20:25:04.

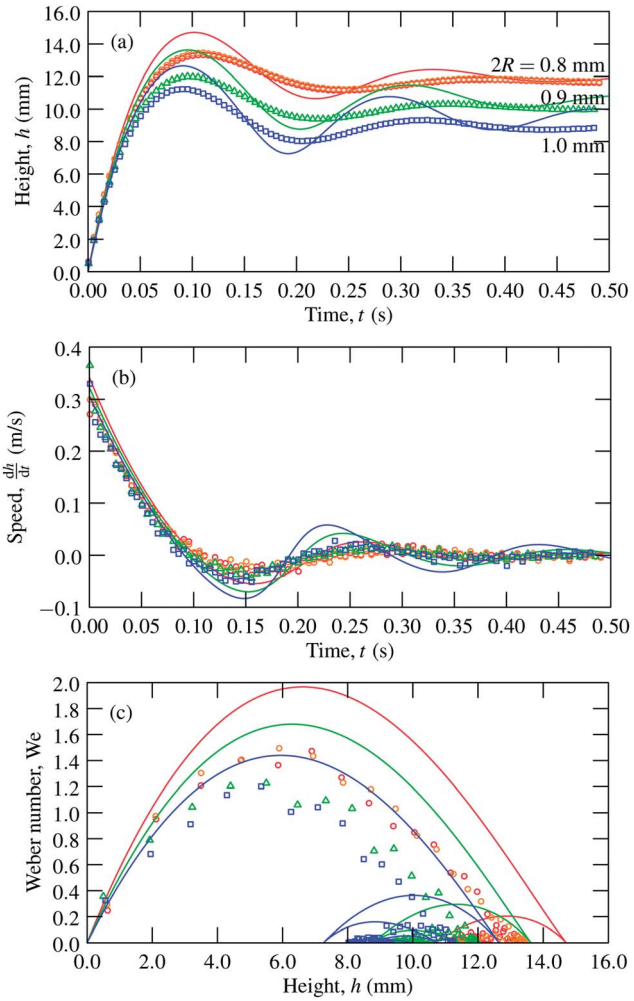

Fig. 1 Capillary rise in 16 mm high tubes with three inner diameters (red and orange circles: 0.8 mm, green triangles: 0.9 mm, blue squares: 1.0 mm): (a) height from the bottom of the tube to the bottom of the meniscus, (b) meniscus speed, and (c) Weber number *versus* rise height. The solid lines show the numerical solution to eqn (7). For clarity, only every hundredth experimental value is shown.

the meniscus. With these contact angles, the capillary driving force is reduced by factors of 0.77 to 0.98, respectively. Models for the dynamic contact angle are available[14,15] and could be used to improve the accuracy of the modeling. The modeling is also simplified by neglecting phenomena at the base of the tube,[11,16] the dynamics of the initial formation of a curved meniscus,[3] the dynamics of viscous boundary layer growth,[17] and variation in the velocity profile from the base to the meniscus.[5,16,18] Due to the lower driving force and other losses, the maximum height achieved and the amplitude of the oscillations are lower in the experiments than in the model. As expected, We* increases with decreasing tube diameter (Fig. 1c). The amplitude of the oscillations decreases with decreasing diameter, indicating an increasing role of viscous dissipation. The narrow range of radii (0.8 to 1.0 mm) in these experiments is optimal for studying the kinetic energy in the inertial regime under terrestrial conditions: We* falls below 1 with wider tubes (Fig. 1c), and the filling regime becomes viscous with narrower tubes. To maintain a focus on primarily inertial filling dynamics, short tubes with 0.8 mm diameters were used for the subsequent experiments rather than narrower tubes that could have a higher We*. As shown in Fig. 1c, We* is 1.4 when h is near 5 mm for a 0.8 mm diameter.

Fig. 2 shows a representative experiment with a nearly-optimal tube height of 4.7 mm. The movement of several interfaces is illustrated in Fig. 2 by showing the recorded brightness along the line down the middle of the tube over time. The dark band along the bottom of the figure indicates the external meniscus around the base of the tube. When the ether touches the bottom of the tube, the flat liquid surface simultaneously wets the inside and outside of the tube wall and rises. The internal meniscus rises faster than the external meniscus, as also recently reported by Andrukh *et al.*[19] As a result, the bottom of the internal meniscus can be seen above the top of the external meniscus (point 1 in Fig. 2) before the external meniscus reaches its equilibrium position. The liquid inside the tube continues to rise, and the top of the internal meniscus reaches the top of the tube at point 2 in Fig. 2. As shown by sequence (a) in Fig. 2, the meniscus becomes flat at point 3, inverts, forms a parabolic shape, and the tip of the meniscus rises. Next, with the tip remaining at a constant height, the liquid bulges out radially. The ether then rises up again, reaches a maximum height, then retracts downward while bulging outward and over the upper edge of the tube. The liquid then wets the external wall (point 4) and some liquid slides down while the liquid inside the tube continues to move downward (sequence (b) in Fig. 2) until it reaches a minimum height (point 5). This continued downward motion after meniscus inversion was also observed by Siegel.[2] The liquid inside the tube then oscillates vertically, as anticipated but not observed by Siegel.[2] As shown in sequence (c) in Fig. 2, the meniscus inverts several times. During the first two subsequent inversions (starting immediately after point 6, which is the second time the meniscus is flat), the tip of the inverted meniscus oscillates quickly in a manner similar to the early stages of the first inversion, but the liquid bulge does not wet the external surface. Eventually the motion of the liquid column dampens, coming to rest (Fig. 2d) within 0.25 s, which is $0.5R^2/\nu$.

The liquid bulge at the top of the tube wets the upper external surface of the tube to achieve a lower-energy configuration that is similar to the shape of a large sessile drop on the tip of a fiber.[20] On the top of a hollow tube, unlike a solid cylinder, the equilibrium shape cannot persist because the higher pressure in the liquid causes it to return downward. However, the liquid that spreads onto the external surface of the tube remains there. After the meniscus initially inverts, the liquid first wets the flat top surface of the tube (thickness 50 μm) when the contact angle at the base of the inverted meniscus with respect to the plane of the top surface locally exceeds the equilibrium contact angle θ_c. If the contact angle later exceeds $\pi/2 + \theta_c$, the liquid also wets the external side wall. As shown in sequence (b) of Fig. 2, $\theta_c \approx 20°$. Considering the dynamics of the capillary filling and wetting processes, we note that the liquid must wet the tube's surface faster than it retreats back

Published on 13 March 2014. Downloaded by University of Alberta on 11/05/2014 20:25:04.

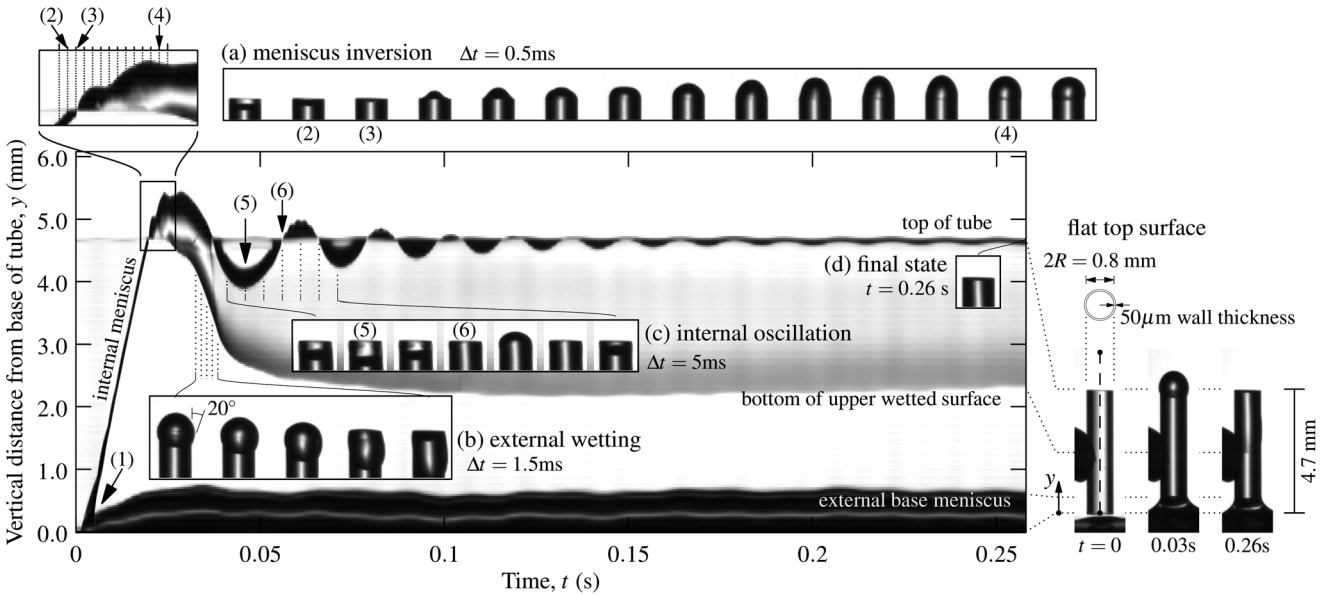

Fig. 2 Stages of the capillary rise in a 4.7 mm high tube with a 0.8 mm inner diameter as illustrated by the recorded brightness along the middle of the tube (dashed line in image of tube at $t = 0$) as a function of time. Sequence (a) shows the inversion of the internal meniscus, sequence (b) shows the descent of the liquid bulge along the external upper surface of the tube, and sequence (c) shows one period of the subsequent oscillation of the liquid column. The final state is shown in (d). The numbers indicate key events that are described in the text.

into the tube to leave behind a wetted upper surface, as it does in our experiments.

Experiments with different capillary tube heights show how the behavior depends on the Weber number. Several tubes, including the previous 4.7 mm tube, were cut with a dicing saw (Diamond Touch, USA). The results with different tube heights are summarized in Fig. 3. Variation in the kinetic energies achieved at the tops of these tubes and the corresponding heights in a tall tube (Fig. 1) is due to the initial wetting process at the base of the tube. To compute the Weber number, we use the rise speed when the top of the internal meniscus reaches the top of the tube (*i.e.* point 2 in Fig. 2, which is before the meniscus starts to flatten) and neglect the details of the initial conditions and how they affect the speed at point 2. Over the range of tube heights we examined, three outcomes occur. The liquid wets the upper external surface of the tube when $1.2 \lesssim We \lesssim 1.8$. Weber numbers above 1.8 were not achieved and the behavior with We > 1.8 is not known. A critical Weber number for external wetting that is approximately one supports the choice of definition for the Weber number: for the experimental conditions the kinetic energy is only enough to form a liquid sphere with about the same radius as the tube. This critical Weber number also indicates that the balance between kinetic energy and surface energy determines when external wetting occurs at the conditions of our experiments (mainly inertial filling dynamics). In comparison to the increase in surface energy, the gain in gravitational potential energy during meniscus inversion and the energy dissipated through viscous losses are small. For $0.6 \lesssim We \lesssim 1$, the meniscus inverts but the liquid does not wet the external surface of the tube. At $We \approx 0.1$, the available kinetic energy is insufficient to invert the meniscus. Since only gravity opposes further rise of the liquid before the meniscus inverts, the critical Weber number for meniscus inversion depends on the Bond number (and the ratio h/R due to the definition of We).

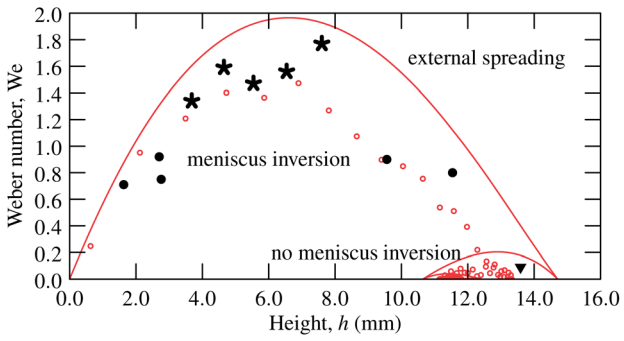

Fig. 3 Weber number as a function of the meniscus height in long and short capillary tubes with a 0.8 mm inner diameter. For reference, the open symbols show the Weber number during one experiment in a tall tube (Fig. 1). The filled symbols show the Weber numbers achieved in experiments with short tubes (1.6, 2.7, 2.8, 3.7, 4.7, 5.5, 6.5, 7.6, 9.6, 11.5, and 13.6 mm). The symbol type indicates the outcome: meniscus inverts but remains pinned (disk), meniscus inverts and spreads on the external surface (star), and meniscus does not invert (triangle). The solid line shows the numerical solution to eqn (7).

To conclude, we have shown that ether rising by capillary action can spread onto the upper external surface of a short tube when the rising liquid reaches the top of the tube. This phenomenon is a consequence of two factors: the high kinetic energy of the rising liquid and the low contact angle of the liquid on the tube. For inertial rise dynamics, in which viscous forces are small, the ratio of the kinetic energy of the liquid and the surface energy of a spherical drop determines whether

 This journal is © The Royal Society of Chemistry 2014

Published on 13 March 2014. Downloaded by University of Alberta on 11/05/2014 20:25:04.

a sufficient amount of liquid is ejected above the tip of the tube for external wetting to occur. When viscous losses cannot be neglected, the analysis would have to account for these losses during meniscus inversion that would reduce the energy that is available to form a liquid–air surface. The maximum possible ratio of the kinetic and surface energies is limited by liquid properties, and the maximum We that we achieve is 1.8. Therefore, the behavior of the liquid when the kinetic energy exceeds the surface energy by one or more orders of magnitude remains an open question that could be studied by experiments in microgravity. To achieve high kinetic energies during inertial filling in microgravity, the Ohnesorge number must be decreased together with the Bond number to ensure that viscous forces remain small. The shape of the tube cross-section is another parameter that can be studied since we have also observed spreading onto the external surface of a square tube.[21] The results of our experiments suggest new possibilities for capillary phenomena, especially in microgravity environments where high kinetic energies can be achieved, and emphasize the importance of considering the kinetic energy of the liquid when modeling such systems.

We thank P. Mendez and the Canadian Centre for Welding and Joining (CCWJ) for their assistance and the use of their high-speed imaging equipment. Funding from NSERC for O. S. is gratefully acknowledged.

References

1 J. Maxwell, *Encyclopædia Britannica*, 1911, 11th edn, vol. V, pp. 256–275.
2 R. Siegel, *J. Appl. Mech.*, 1961, **83**, 165–170.
3 M. Stange, M. Dreyer and H. Rath, *Phys. Fluids*, 2003, **15**, 2587–2601.
4 A. Wollman and M. Weislogel, *Exp. Fluids*, 2013, **54**, 1499.
5 B. Zhmud, F. Tiberg and K. Hallstensson, *J. Colloid Interface Sci.*, 2000, **228**, 263–269.
6 N. Fries and M. Dreyer, *J. Colloid Interface Sci.*, 2008, **327**, 125–128.
7 J. Jurin, *Philos. Trans. R. Soc. London*, 1717, **30**, 739–747.
8 E. Washburn, *Phys. Rev.*, 1921, **17**, 273–283.
9 C. Bosanquet, *Philos. Mag.*, 1923, **45**, 525–531.
10 D. Quéré, *Europhys. Lett.*, 1997, **39**, 533–538.
11 D. Quéré and E. Raphaël, *Langmuir*, 1999, **15**, 2679–2682.
12 S. Das and S. Mitra, *Phys. Rev. E: Stat., Nonlinear, Soft Matter Phys.*, 2013, **87**, 063005.
13 P. Waghmare and S. Mitra, *Microfluid. Nanofluid.*, 2012, **12**, 53–63.
14 T.-S. Jiang, S.-G. Oh and J. Slattery, *J. Colloid Interface Sci.*, 1979, **69**, 74–77.
15 A. Saha and S. Mitra, *J. Colloid Interface Sci.*, 2009, **339**, 461–480.
16 S. Levine, J. Lowndes, E. Watson and G. Neale, *J. Colloid Interface Sci.*, 1980, **73**, 136–151.
17 F. M. White, *Viscous Fluid Flow*, McGraw-Hill, 1974.
18 J. Szekely, A. Newmann and Y. Chuang, *J. Colloid Interface Sci.*, 1971, **35**, 273–278.
19 T. Andrukh, D. Monaenkova, B. Rubin, W.-K. Lee and K. Kornev, *Soft Matter*, 2014, **10**, 609–615.
20 J. Du, S. Michielsen and H. Lee, *Langmuir*, 2010, **26**, 16000–16004.
21 O. Shardt, P. Waghmare, J. Derksen and S. Mitra, 2013, arXiv:1310.3743.